Author's response to comments from Anonymous Referee #2:

Aerosol–cloud interactions influence the climate response to AMOC weakening

by Ryan Vella & Ulrike Lohmann

We thank the editor and referees for taking the time to review our manuscript and for the valuable feedback.

Here, the comments from Anonymous Referee #2 (from June 22, 2026) are reproduced in black, while our responses are presented in blue.

We thank the referee for the constructive and detailed review. Before the detailed responses, we note important changes made during revision. First, we identified and corrected a coding error in the coupling between the land surface scheme and the interactive dust emission scheme, in which regional scaling factors were passed incorrectly to the emission calculation, overestimating dust fluxes. The bug was fixed, the model was retuned, and both simulations were rerun. All quantitative values in the revised manuscript have been updated. This correction changed magnitudes only, and the sign and mechanism of the aerosol and cloud-microphysical responses are unchanged, including the hemispheric aerosol redistribution, the two-pathway microphysical response, and the regional structure of the cloud radiative anomalies.

Additionally, and independently of this correction, we replaced the CRE-based attribution with an ISCCP-simulator cloud radiative kernel decomposition (Zelinka et al., 2012a, b) and included double-call aerosol radiation diagnostics, prompted by this referee's comments on clear-sky masking and by Referee #1's comments on isolating the aerosol effect. This new analysis revises the interpretation of the results. While the cloud radiative response is strong regionally, its opposing contributions largely cancel, resulting in $+0.19\,\mathrm{W\,m^{-2}}$. The global radiative response is instead dominated by the dust direct effect and the surface albedo term, which together reinforce rather than offset the AMOC-induced cooling ($-0.87\,\mathrm{W\,m^{-2}}$). The text has been revised accordingly, and the quantitative details are given in our responses to the relevant comments below.

Main Comments

1. Cloud radiative effects (CRE; Fig. 8) do not isolate the radiative consequences of cloud changes (L337), assuming CRE is calculated as the difference between the all-sky and clear-sky top-of-atmosphere radiation anomalies. Calculating the actual cloud feedbacks rather than the CRE may significantly change the authors' finding that cloud changes produce a negative cloud feedback in response to AMOC weakening. A positive SW CRE anomaly (Fig. 8) can occur even when there are no cloud changes, due to changes in other variables. For the experiments here, there is a large increase in sea-ice area (Figure 1,

bottom left) that will increase the surface albedo. As a result, a cloud that has a large SW cooling CRE in the control experiment will have a much smaller SW cooling CRE when the ocean surface below is replaced with sea ice in the AMOC decline experiment, because even in clear-sky conditions the sea ice will reflect a large fraction of incoming SW radiation. This will produce a positive polar/subpolar SW CRE anomaly for the AMOC decline v. preindustrial control even in the absence of any cloud changes, solely due to surface albedo changes. These cloud masking effects are discussed further in Soden et al. (2008; https://doi.org/10.1175/2007JCLI2110.1), and can result not only from surface albedo changes, but also from changes in water vapor and atmospheric temperature.

To isolate the cloud feedback that results from cloud changes alone, and not changes in other variables, I recommend using a cloud feedback analysis. Options here would be the radiative kernel approach from Soden et al. (2008), the cloud radiative kernel method from Zelinka et al. (2012; DOI: 10.1175/JCLI-D-11-00248.1), or the APRP method (although this one only calculates the SW cloud feedback). I think the best approach would be the cloud radiative kernel method, which directly calculates cloud feedbacks due to changes in cloud amount, altitude, and optical depth, but the authors would need to run their experiments with the COSP satellite simulator active to provide the necessary variables for this. There's code for the cloud radiative kernel and APRP methods at Mark Zelinka's Github (https://github.com/mzelinka), and code for the standard radiative kernel approach from Tyler Janoski (Janoski et al., 2025; https://github.com/tyfolino/climkern). One other note is that when taking the global-mean SW cloud feedback change, it might be worth also calculating this while excluding deep convective clouds, which have compensating LW cloud feedbac k changes.

We thank the reviewer for this detailed and constructive recommendation, which we have adopted in full. The referee is entirely correct that the CRE does not isolate the cloud feedback and is contaminated by clear-sky masking, and that the large sea-ice increase in our experiment produces a positive shortwave CRE anomaly over the Arctic and along the sea-ice margins through the surface-albedo masking mechanism the referee describes, independent of any cloud change.

Following the referee's primary recommendation, we reran both simulations with the COSP/ISCCP satellite simulator active and applied the cloud radiative kernel method of Zelinka et al. (2012a, b) to the simulated cloud-top-pressure–optical-depth histograms, using the kernels and code from the referenced repository. This decomposes the cloud feedback into contributions from cloud amount, altitude, and optical depth, free of the masking that affects the CRE. We additionally applied the APRP method (Taylor et al., 2007) to isolate the shortwave surface-albedo term, and implemented a double-call (aerosol-free) radiation diagnostic to quantify the aerosol direct effect, so that the surface-albedo, aerosol-direct, and cloud contributions are separated.

The masking-free analysis substantially revises our interpretation. Of the raw net CRE anomaly ($+0.86\,\mathrm{W\,m^{-2}}$), only $+0.19\,\mathrm{W\,m^{-2}}$ is a genuine cloud radiative adjustment, itself a near cancellation of optical-depth ($+0.37$), altitude ($+0.16$), cloud-amount (-0.22) and residual ($-0.11\,\mathrm{W\,m^{-2}}$) terms; the remainder is clear-sky masking by the expanded sea ice and the enhanced dust. As the referee anticipated, the positive shortwave CRE anomaly over the Arctic and along the sea-ice margins is surface-albedo masking rather than a cloud change, whereas over the subpolar North Atlantic the cloud increase dominates and both the CRE and the kernel-corrected adjustment are negative. With the surface-albedo term ($-0.83\,\mathrm{W\,m^{-2}}$, APRP) and the aerosol direct effect ($-0.23\,\mathrm{W\,m^{-2}}$) isolated, the top-of-atmosphere response is dominated by these two cooling terms, which reinforce rather than offset the AMOC-induced cooling. Section 3.4 and Fig. 9 have been revised accordingly, and the CRE is now used only to describe the spatial structure of the response.

Following the referee's suggestion, we also excluded the deep convective (high-top, high-optical-depth) bins from the kernel calculation. This reduces the global-mean shortwave cloud adjustment from $+0.49$ to $+0.12\,\mathrm{W\,m^{-2}}$ and the net adjustment from $+0.19$ to $+0.07\,\mathrm{W\,m^{-2}}$, confirming that the deep convective regime carries compensating shortwave and longwave changes and that the genuine cloud feedback is small.

2. It would be helpful to see a more specific discussion of why this study's cloud feedback may differ from previous studies of the cloud response to the AMOC decline. Specifically, why is there a negative SW cloud feedback here (if this persists in the new feedback analysis), in contrast to a positive SW cloud feedback identified in previous literature (e.g., Zhang et al. (2010; https://doi.org/10.1175/2009JCLI3118.1), He et al. (2017; https://doi.org/10.1175/JCLI-D-16-0581.1), Trossman et al. (2016; https://doi.org/10.1002/2016GL Lin et al. (2019; https://doi.org/10.1029/2019GL083084), and Hahn et al. (2025; https://doi.org/10.1175/JCLI-D-24-0752.1))? In what ways does this model represent aerosols differently from other models that have produced opposite results?

We thank the referee for this important question and for the additional references, which we now cite. We would first clarify a point that the masking-free analysis makes clear: over the subpolar North Atlantic our result is in fact consistent with the studies the referee lists, not opposed to them. There, the shortwave cloud radiative response is a cooling of about -3 to $-4\,\mathrm{W\,m^{-2}}$ (Figs. 8a and 9b), reflecting the increase in low-cloud cover and cloud brightening over the cooled ocean that reinforces the surface cooling, exactly as reported by Zhang et al. (2010); He et al. (2017); Trossman et al. (2016); Lin et al. (2019); Hahn et al. (2025). We agree with this regional low-cloud response.

The distinction is in the global mean, and it involves a process that the cited studies do not examine. In our simulations, the enhanced Saharan dust acts as an ice-nucleating particle in mixed-phase clouds, promoting glaciation and the WBF process, which depletes cloud water and reduces cloud optical thickness. This dust-driven thinning contributes, together with the thermodynamic loss of condensate in cold clouds and the reduced occurrence of the deepest convective tops, to the positive optical-depth term of the kernel decomposition ($+0.37\,\mathrm{W\,m^{-2}}$), which opposes the subpolar low-cloud brightening and the increased cloud amount, so that the global-mean cloud radiative adjustment is small ($+0.19\,\mathrm{W\,m^{-2}}$, or $+0.07\,\mathrm{W\,m^{-2}}$ excluding deep convective clouds) rather than a strong feedback of either sign. Isolating the dust-driven share of this term would require an additional hosing experiment with ice-nucleating particle concentrations held at control values, which is beyond the present design; we state this explicitly in Sect. 3.4. In the masking-free framework the strong damping signal of our original CRE-based analysis therefore does not persist: the raw shortwave CRE anomaly ($+1.15\,\mathrm{W\,m^{-2}}$) reduces to a masking-free shortwave cloud adjustment of $+0.49\,\mathrm{W\,m^{-2}}$, much of the apparent global signal having reflected surface-albedo and aerosol clear-sky masking, while the genuine subpolar cloud response remains a shortwave cooling in agreement with previous work.

Regarding aerosol representation, ICON-HAM differs from most of the models in the cited studies in two respects central to this result. First, it carries a prognostic aerosol population (the M7 modal scheme) coupled to a two-moment cloud microphysics scheme, so that cloud droplet and ice-crystal number concentrations respond interactively to the simulated aerosol rather than being prescribed or diagnosed from a fixed climatology. Second, mineral dust acts as an interactive ice-nucleating particle for immersion and contact freezing, so that the AMOC-driven dust increase feeds directly into ice-phase cloud microphysics. It is this second pathway, the interactive coupling from mineral-dust emission through ice-nucleating particles to mixed-phase glaciation and the WBF reduction of cloud optical depth, that was not assessed in the cited studies, which examined the macrophysical and thermodynamic cloud response to AMOC weakening rather than aerosol-driven ice-phase microphysics. We have added this comparison to Sect. 3.4.

3. Can the authors discuss the extent to which the results may be state-dependent? This study's experiments use preindustrial CO2 forcing and prescribe changes in SSTs and SICs from NAHosMIP experiments that impose an AMOC decline in a preindustrial climate. However, in reality the AMOC will decline in an environment with increasing CO2 concentrations. As an alternative to the NAHosMIP protocol, other studies have assessed the impact of the AMOC decline by comparing experiments with increased CO2 to experiments with both increased CO2 and freshwater removal that produces a constant AMOC strength (e.g. Liu et al., 2020; https://doi.org/10.1126/sciadv.aaz4876). Comparison of these future CO2 experiments with preindustrial NAHosMIP experiments has demonstrated state-dependent AMOC impacts (Bellomo and Mehling, 2024, also cited by the authors). I'm wondering how the AMOC-induced cloud response might differ when the background state has increased CO2 concentrations? Perhaps this would reduce the background cloud amount in the North Atlantic, so that there would be a smaller capacity for AMOC-induced dust changes to reduce cloud optical depth. On the other hand, there may be a larger reduction in North Atlantic precipitation for an AMOC decline in a future climate (Bellomo and Mehling, 2024), reducing wet deposition and increasing the impact of dust changes.

We thank the referee for raising state-dependence, and for the Liu et al. (2020) reference. We would first clarify the experimental design, as the referee's summary describes a preindustrial background. The atmospheric background state of our simulations is in fact present-day: the prescribed SST climatology is the year-2015 multi-model mean under SSP5-8.5, anthropogenic and biomass-burning emissions are held at 2015 levels, and greenhouse gas concentrations follow the CMIP6 historical dataset. Only the AMOC-related SST and sea-ice anomalies are taken from the EC-Earth3 NAHosMIP hosing experiment, which was itself performed on a pre-industrial background. Our configuration therefore already places the AMOC-driven anomaly on a present-day, warmer-than-preindustrial base rather than on a preindustrial one; we have made this explicit in Sect. 2.

We agree the response is likely state dependent, and that our fixed background design cannot capture a future in which the mean climate warms as the AMOC declines. The two pathways the referee raises act in opposite directions. A warmer background reduces subpolar North Atlantic supercooled cloud water, damping the glaciation and cloud thinning driven by dust, whereas a larger North Atlantic precipitation reduction (Bellomo and Mehling, 2024) would suppress wet scavenging and amplify the aerosol response. Resolving the net sign would require dedicated experiments, for example applying the hosing anomaly on a warm SSP background or adopting the constant AMOC differencing of Liu et al. (2020). We therefore flag this as a limitation and a direction for future work rather than attempting to evaluate it here.

4. Can the authors please explain some points of the experimental design:

Figure 1, bottom right suggests that the prescribed, AMOC-induced SST/SIC anomaly experiments have land surface temperatures fixed to the preindustrial control conditions, but large surface temperature changes over land in Figure 2 indicate that land temperatures are not prescribed. Please clarify whether land is interactive in the experimental design section and consider changing this schematic.

The land surface temperature is not prescribed. The only prescribed surface boundary conditions are sea surface temperature and sea ice concentration. Over land, the surface temperature and surface energy balance are computed interactively, so the large land temperature anomalies in Fig. 2 are the freely evolving atmosphere–land response to the imposed ocean perturbation. The land runs in the jsbach_lite configuration, in which vegetation phenology and albedo follow a fixed climatology and the carbon cycle is disabled, but this simplification does not prescribe the land temperature. The AMOC-driven increase in North African dust emission is in turn driven by the interactively simulated surface winds. The Fig. 1 caption has been updated accordingly.

Which two periods from the EC-Earth hosing experiment are taken to calculate and prescribe SIC and SST anomalies?

The control state is averaged over the first decade of the 140-year hosing integration (model years 1-10), during which the AMOC remains at its pre-industrial strength of ~ 17.5 Sv before responding to the imposed freshwater flux, and the weakened state over the final 12 years (model years 129-140), when the AMOC has declined to ~ 7.0 Sv. The window selection follows the approach of Meccia et al. (2024) for this simulation (Fig. R1, adapted from Fig. S1 of that study).

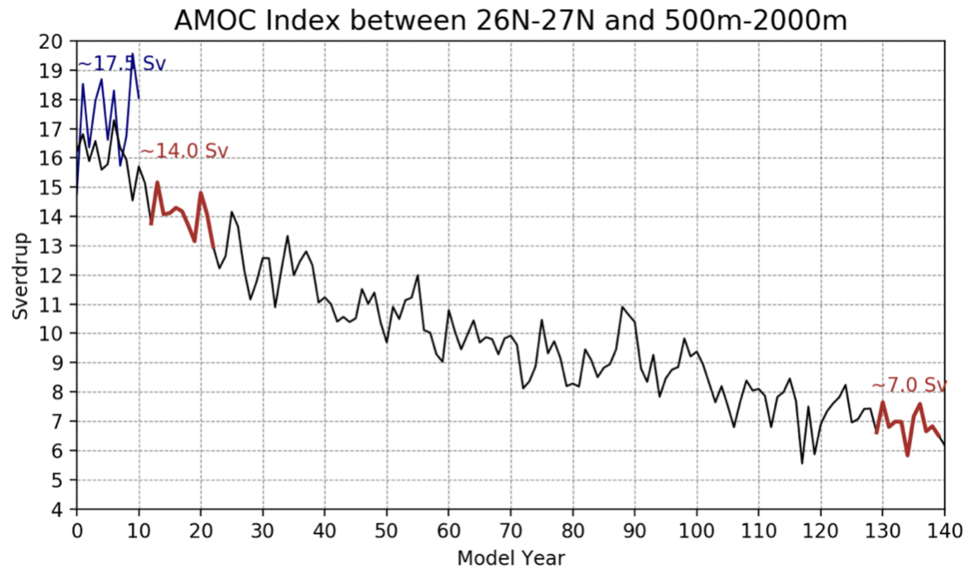

Figure S1: Annual maximum Atlantic meridional streamfunction around 26.5ºN and between 500 and 2000 m depth throughout the 140-year coupled simulation with water hosing applied in the North Atlantic and the Arctic. Colours highlight the periods selected as boundary conditions for the three sets of AMIP-like experiments: the pre-industrial (blue; ctrl) and the weak (-20%; a14) and strong (-60%; a07) AMOC reduction with respect to the control.

Figure R1. Annual maximum Atlantic meridional streamfunction at $\sim 26.5°$N between 500 and 2000 m depth throughout the 140-year coupled EC-Earth3 simulation with freshwater hosing applied in the North Atlantic and the Arctic. Colours indicate the averaging windows used to derive the boundary conditions, the control state (~ 17.5 Sv, blue) and the strongly weakened state (~ 7.0 Sv, red). Taken from Meccia et al. (2024).

Why not compare the hosing experiment with a preindustrial experiment (with no hosing) to calculate SIC and SST anomalies?

The anomalies are in fact taken against the unperturbed, strong-AMOC state, which corresponds to the pre-industrial circulation the referee has in mind. In the EC-Earth3 integration the AMOC begins at its full pre-industrial strength (~ 17.5 Sv) and is driven by the sustained 0.3 Sv freshwater flux to a new quasi-equilibrium at ~ 7.0 Sv. Our ΔSST and ΔSIC are the difference between these two quasi-equilibrated states, so the reference is the full-strength-AMOC pre-industrial ocean surface, exactly as the referee suggests.

We take this difference within a single continuous coupled integration, rather than against a separately initialised pre-industrial control run, by design. Both states share the same model, resolution, external forcing, and long-term drift, so their difference isolates the AMOC-weakening signal and is not influenced by inter-simulation drift, initialisation differences, or independent sampling of internal variability that would enter a difference taken across two separate simulations. Each state is a quasi-equilibrated mean, so the anomaly represents the equilibrium ocean-surface response to AMOC weakening rather than a transient snapshot. The reference window has already received roughly a decade of freshwater input, but its imprint on SST and sea ice before the circulation responds is small, as reflected in the unchanged overturning strength during this period (Fig. R1). This construction follows the NAHosMIP protocol of Jackson et al. (2023).

Other Comments:

Abstract: The authors state that the negative feedback from reduced cloud optical depth more than offsets the positive feedback from increased cloud amount. To highlight the significance of this result, I suggest adding somewhere in the abstract that previous studies have instead found a positive cloud feedback in response to AMOC weakening—this is a key difference of the present study.

We thank the referee for this suggestion. Following our masking-free reanalysis (Comment 1), the abstract has been substantially revised and the sentence quoted here no longer appears. The genuine global-mean cloud radiative adjustment is now small ($+0.19\,\mathrm{W\,m^{-2}}$), a near cancellation between subpolar low-cloud brightening and optical thinning of mixed-phase and ice clouds, to which dust-driven glaciation contributes, rather than a net cloud feedback of either sign. We agree that the contrast with previous work strengthens the abstract, and have added a sentence noting that this small global-mean cloud feedback differs from previous studies of AMOC weakening, in which cloud changes contribute a net radiative feedback on the surface response, and that in our simulations the global radiative response is instead set by the dust direct effect and the albedo of expanded sea ice and snow.

Figure 1: Suggest adding color bars to these plots. Otherwise the sign of the SST and SIC changes is unclear.

Figure 1 is intended as a schematic of the experimental design rather than a quantitative presentation of the forcing, so the ΔSST and ΔSIC tiles are illustrative. The full signed fields, with colour bars, are shown in Fig. S1.

L20: Recent literature has found that heat fluxes, rather than freshwater fluxes, are the main cause of projected AMOC weakening (e.g., Couldrey et al., 2022, Fig. 3; https://doi.org/10.1007/s00382-022-06386-y).

We agree, and this point was raised independently by Referee #1. The opening paragraph has been rewritten so that anthropogenic forcing acts on upper-ocean buoyancy through both freshwater and thermal pathways, and it now cites Couldrey et al. (2023) for the finding that heat flux anomalies rather than freshwater fluxes dominate the projected weakening.

L40: When isolating the effect of the AMOC decline alone (rather than the combined effect of GHG warming and AMOC cooling), this surface cooling and positive low-cloud feedback is not limited to the warming hole in the subpolar North Atlantic; rather, it extends to the North Atlantic midlatitudes and subtropics. Other studies that show this positive shortwave cloud feedback include Zhang et al. (2010; https://doi.org/10.1175/2009JCLI3118.1), He et al. (2017; https://doi.org/10.1175/JCLI-D-16-0581.1), Lin et al. (2019; https://doi.org/10.1029/2019GL083084), and Hahn et al. (2025; https://doi.org/10.1175 D-24-0752.1).

We thank the referee for this clarification and for the references. We agree that, when the AMOC decline is isolated from greenhouse warming, the surface cooling and the accompanying positive low-cloud shortwave feedback are not confined to the subpolar warming hole but extend across the North Atlantic midlatitudes and into the subtropics. Our results are consistent with this broader extent: the low-cloud increase (Fig. 5a) is a broad band spanning the subpolar and midlatitude North Atlantic, and the associated shortwave cooling (Fig. 8a) follows the same pattern rather than being confined to the warming hole. We have revised the text in Sect. 3.4 to state this explicitly, and cite the relevant papers.

L106: To what extent do the authors expect differences between the simulations' short, 10-year climatologies to result from differences in internal atmospheric variability, in addition to AMOC differences?

This is an important consideration, and our experimental design substantially limits it. Because both simulations are forced with a perpetually repeating monthly SST and sea-ice climatology, the ocean-coupled modes that dominate low-frequency internal variability in coupled models, such as ENSO and Atlantic multidecadal variability, are absent by construction and identical between the two runs in their boundary forcing. The residual internal variability is atmospheric and land-surface in origin, with decorrelation timescales of days to at most a season, far shorter than the multidecadal ocean modes removed by the prescribed forcing, so a 10-year integration provides a much larger effective sample than the same period in a coupled framework. The aerosol life cycle operates on these same short timescales, and the oxidant and ozone fields are prescribed rather than computed interactively, so there is no slowly equilibrating chemistry or biogeochemical reservoir that would require a multidecadal spin-up; the aerosol distribution adjusts rapidly to the imposed circulation and reaches a stable climatology well within the analysis period, with the first three months discarded as spin-up. Finally, the stippling in all map figures tests each grid cell against precisely this fast internal noise at the 95 % confidence level, and the temperature-binned composites (Figs. 7 and S6) are constructed from daily and sub-daily gridpoint samples with correspondingly narrow ± 2 SEM envelopes.

L251-253: It would be helpful for the reader to explicitly reference cloud cover vs. LWP here—like "triggers additional cloud formation, increasing mid- and high-cloud cover, but the reduced absolute moisture leaves less moisture available to condense within each cloud, reducing LWP and IWP." This would tie things back better to the intro sentence for this paragraph.

We have revised the sentence to state explicitly that the higher relative humidity increases mid- and high-level cloud cover while the reduced absolute moisture lowers the condensate available per cloud, so that LWP and IWP decrease, tying the mechanism back to the opening sentence of the paragraph.

L269: Why focus on 40-90N? It looks like there are large cloud changes to the south of this in the North Atlantic as well (Figures 5,6), and the dust changes are mainly in the tropics (Figure 4).

This restriction applies only to the temperature-binned microphysical composite of Fig. 7; the aerosol fields (Figs. 3, 4), the macrophysical cloud response (Figs. 5, 6), and the radiative analysis (Figs. 8 and 9) are all shown globally, so the cloud changes south of 40°N, including the tropical ITCZ dipole, are fully presented and discussed.

We focus the microphysical composite on 40–90°N for two reasons. First, this is where the AMOC-driven surface cooling is strongest, so the cloud-phase response is largest and most clearly attributable to the AMOC. Second, it is the region where mixed-phase and ice clouds are widespread at the temperatures required for the dust immersion- and contact-freezing pathway that is central to our result. In the tropics, clouds at these temperatures are deep convective towers in a very different dynamical regime, so a composite that mixed the two would confound the aerosol signal with regime differences within each temperature bin.

Page 16: The discussion of Figure 7 was quite detailed, and I got a bit lost in which of these features are most important when considering the TWP changes, which aren't discussed until the very end of this section. Please consider streamlining this to make it clear how these features are relevant for the main points of the paper.

We agree and have restructured this discussion around the quantity that matters for the paper's main result. The revised section now introduces the TWP changes and their regime structure at the outset, and each subsequent paragraph traces the microphysical chain for one cloud regime, ending at its TWP change, namely the warm-cloud pathway from elevated CCN through suppressed autoconversion to a TWP increase, the mixed-phase pathway from enhanced dust INP through an ICNC increase set by the INP supply and the WBF process to a TWP decrease, and the cold-cloud pathway in which aerosol plays no direct role and the TWP decrease follows from the stability-driven reorganisation of the cirrus population toward warmer cloud tops. The previously duplicated discussion of the cirrus mechanism has been consolidated into a single paragraph, and the discussion is now substantially shorter.

References

Bellomo, K. and Mehling, O.: Impacts and State-Dependence of AMOC Weakening in a Warming Climate, Geophysical Research Letters, 51, e2023GL107 624, https://doi.org/10.1029/2023GL107624, 2024.

Couldrey, M. P., Gregory, J. M., Dong, X., Garuba, O., Haak, H., Hu, A., Hurlin, W. J., Jin, J., Jungclaus, J., Köhl, A., Liu, H., Ojha, S., Saenko, O. A., Savita, A., Suzuki, T., Yu, Z., and Zanna, L.: Greenhouse-Gas Forced Changes in the Atlantic Meridional Overturning Circulation and Related Worldwide Sea-Level Change, Climate Dynamics, 60, 2003–2039, https://doi.org/10.1007/s00382-022-06386-y, 2023.

Hahn, L. C., Lutsko, N. J., Eisenman, I., Luongo, M. T., and Xie, S.-P.: Contribution of AMOC Decline to Uncertainty in Global Warming via Ocean Heat Uptake and Climate Feedbacks, Journal of Climate, 38, 6245–6259, https://doi.org/10.1175/JCLI-D-24-0752.1, 2025.

He, J., Winton, M., Vecchi, G., Jia, L., and Rugenstein, M.: Transient Climate Sensitivity Depends on Base Climate Ocean Circulation, Journal of Climate, 30, 1493–1504, https://doi.org/10.1175/JCLI-D-16-0581.1, 2017.

Jackson, L. C., Alastrué de Asenjo, E., Bellomo, K., Danabasoglu, G., Haak, H., Hu, A., Jungclaus, J., Lee, W., Meccia, V. L., Saenko, O., Shao, A., and Swingedouw, D.: Understanding AMOC Stability: The North Atlantic Hosing Model Intercomparison Project, Geoscientific Model Development, 16, 1975–1995, https://doi.org/10.5194/gmd-16-1975-2023, 2023.

Lin, Y.-J., Hwang, Y.-T., Ceppi, P., and Gregory, J. M.: Uncertainty in the Evolution of Climate Feedback Traced to the Strength of the Atlantic Meridional Overturning Circulation, Geophysical Research Letters, 46, 12 331–12 339, https://doi.org/10.1029/2019GL083084, 2019.

Liu, W., Fedorov, A. V., Xie, S.-P., and Hu, S.: Climate Impacts of a Weakened Atlantic Meridional Overturning Circulation in a Warming Climate, Science Advances, 6, eaaz4876, https://doi.org/10.1126/sciadv.aaz4876, 2020.

Meccia, V. L., Simolo, C., Bellomo, K., and Corti, S.: Extreme cold events in Europe under a reduced AMOC, Environmental Research Letters, 19, 014 054, https://doi.org/10.1088/1748-9326/ad14b0, 2024.

Taylor, K. E., Crucifix, M., Braconnot, P., Hewitt, C. D., Doutriaux, C., Broccoli, A. J., Mitchell, J. F. B., and Webb, M. J.: Estimating Shortwave Radiative Forcing and Response in Climate Models, J. Climate, 20, 2530–2543, https://doi.org/10.1175/JCLI4143.1, 2007.

Trossman, D. S., Palter, J. B., Merlis, T. M., Huang, Y., and Xia, Y.: Large-Scale Ocean Circulation-Cloud Interactions Reduce the Pace of Transient Climate Change, Geophysical Research Letters, 43, 3935–3943, https://doi.org/10.1002/2016GL067931, 2016.

Zelinka, M. D., Klein, S. A., and Hartmann, D. L.: Computing and Partitioning Cloud Feedbacks Using Cloud Property Histograms. Part I: Cloud Radiative Kernels, Journal of Climate, 25, 3715–3735, https://doi.org/10.1175/JCLI-D-11-00248.1, 2012a.

Zelinka, M. D., Klein, S. A., and Hartmann, D. L.: Computing and Partitioning Cloud Feedbacks Using Cloud Property Histograms. Part II: Attribution to Changes in Cloud Amount, Altitude, and Optical Depth, Journal of Climate, 25, 3736–3754, https://doi.org/10.1175/JCLI-D-11-00249.1, 2012b.

Zhang, R., Kang, S. M., and Held, I. M.: Sensitivity of Climate Change Induced by the Weakening of the Atlantic Meridional Overturning Circulation to Cloud Feedback, Journal of Climate, 23, 378–389, https://doi.org/10.1175/2009JCLI3118.1, 2010.